AIR POLLUTION

Total organic carbon measurements reveal major gaps in petrochemical emissions reporting

Megan He[1]†, Jenna C. Ditto[1]‡, Lexie Gardner[1], Jo Machesky[1], Tori N. Hass-Mitchell[1], Christina Chen[1], Peeyush Khare[1]§, Bugra Sahin[1], John D. Fortner[1], Desiree L. Plata[1]¶, Brian D. Drollette[1]#, Katherine L. Hayden[2], Jeremy J. B. Wentzell[2], Richard L. Mittermeier[2], Amy Leithead[2], Patrick Lee[2], Andrea Darlington[2], Sumi N. Wren[2], Junhua Zhang[2], Mengistu Wolde[3], Samar G. Moussa[2], Shao-Meng Li[4], John Liggio[2]*, Drew R. Gentner[1]*

Anthropogenic organic carbon emissions reporting has been largely limited to subsets of chemically speciated volatile organic compounds. However, new aircraft-based measurements revealed total gas-phase organic carbon emissions that exceed oil sands industry–reported values by 1900% to over 6300%, the bulk of which was due to unaccounted-for intermediate-volatility and semivolatile organic compounds. Measured facility-wide emissions represented approximately 1% of extracted petroleum, resulting in total organic carbon emissions equivalent to that from all other sources across Canada combined. These real-world observations demonstrate total organic carbon measurements as a means of detecting unknown or underreported carbon emissions regardless of chemical features. Because reporting gaps may include hazardous, reactive, or secondary air pollutants, fully constraining the impact of anthropogenic emissions necessitates routine, comprehensive total organic carbon monitoring as an inherent check on mass closure.

Gaseous organic compounds are associated with considerable air quality and environmental impacts through exposure to primary emissions (*1*, *2*) and/or after their photochemical reactions and multigenerational oxidative transformations. The latter leads to secondary air pollution, including tropospheric ozone (*3*) and secondary organic aerosol (SOA)—a principal component of particulate matter ($PM_{2.5}$) (*4*) linked to major health and climate effects (*5*, *6*). Governments often mandate monitoring and reporting to develop emissions inventories to track pollutant sources and target regulatory actions. However, emissions monitoring and reporting have historically relied on discrete subsets of compounds limited to smaller hydrocarbons, with the underlying assumption that they cover the majority of carbon and/or reactivity. In reality, the chemical complexity of anthropogenic carbonaceous emissions spans a highly diverse range of molecular sizes and functionalities, including volatile organic compounds (VOCs), intermediate-volatility organic compounds (IVOCs), and semivolatile organic compounds (SVOCs) (*7*, *8*) as well as lower-volatility species in primary organic aerosol. For most research, monitoring, and reporting programs, measuring all of these individual species is not technically, logistically, or financially feasible for either a region or industrial facilities. Consequently, only a subset of carbonaceous compounds (usually VOCs) is routinely measured and/or reported as emissions.

This is particularly relevant for the oil and gas sector, for which emitted hydrocarbons can span the entire VOC-to-SVOC volatility range depending on the deposits, from light hydrocarbons in natural gas reservoirs (*9*) up to SVOCs in the case of unconventional petroleum resources (*10*). Over recent decades, global petroleum production has shifted to more unconventional sources, including heavy oil and bitumen deposits, which together are expected to account for up to 40% of global oil production by 2040 (*11*). One such deposit is Canadian oil sands, which contains an estimated 1.7 trillion barrels of oil and currently produces ~3 million barrels of crude bitumen daily (*12*, *13*), comprising the majority of Canadian oil production (*14*). This global transition to unconventional resources, and the associated diversity of emissions, presents challenges for traditional speciated VOC-focused approaches.

These challenges are evident for Canadian oil sands extraction and processing regions, where a variety of carbonaceous pollutants and their subsequent secondary products have been observed downwind of facilities (*3*, *10*, *15*–*17*). Yet limited reported emissions of individual carbonaceous species cannot be reconciled with incomplete existing emissions measurements (*15*) or explain the diverse magnitude of secondary products observed (*10*, *16*). Hence, these vast oil sands operations provide a key opportunity to examine one major petrochemical sector's reporting discrepancies caused by wide organic compound ranges that are often overlooked by traditional means but affect atmospheric chemistry, leading to SOA and ozone and their associated human and ecosystem health effects.

Using new measurements of total gas-phase organic carbon (TC) emissions from oil sands facilities, we conducted the first carbon closure experiments for any industrial source. These measurements present a powerful approach to capture the full range of organic pollutants, which we used to derive top-down facility-wide TC emissions from surface and in situ oil sands mining operations for comparison with bottom-up industry-reported values. Supported by the most chemically detailed characterization of their emissions to date as well as complementary laboratory experiments, this study demonstrates the magnitude and impact of unmonitored organic gases on emissions reporting, including IVOCs and SVOCs (I/SVOCs) from non–combustion-related sources, highlighting the need to advance routine emissions reporting and monitoring beyond traditional VOCs.

Results

Total observed organic carbon emissions greatly exceed reported emissions

TC concentrations (excluding methane) were measured in April to July 2018 across box-shaped (n = 16) and downwind flights (n = 14) (table S1) in the Athabasca oil sands region (Alberta, Canada) by using an aircraft deployment of paired carbon dioxide (CO_2) analyzers, one with a catalyst-outfitted inlet to convert all organic gases to CO_2 (*18*). Elevated TC concentrations [>0.2 parts per million by carbon (ppmC)] were observed across facility locations and types (six surface mining and six in situ) (examples are given in Fig. 1A), from which emission rates were derived for each facility by using the top-down emission rate retrieval algorithm (TERRA) (Fig. 1, fig. S3, and table S2) (*19*–*21*). Surface mining sites use shallow oil sands reserves, whereas in situ operations extract bitumen from deeper deposits by using various methods, including steam-assisted gravity drainage (*22*).

Observed hourly emission rates varied between facilities (2 to 40 tonnes C $hour^{-1}$) but were generally comparable between surface mining and in situ facilities (Fig. 1B and fig. S3) despite substantial differences in on-site operations and typically lower crude bitumen production rates for individual in situ operations. When normalizing the annualized emission rates by reported facility-level annual crude bitumen production (*23*), the average TC emission intensity (excluding methane) across

[1]Department of Chemical and Environmental Engineering, Yale University, New Haven, CT, USA. [2]Air Quality Research Division, Environment and Climate Change Canada, Toronto, ON, Canada. [3]National Research Council Canada, Ottawa, ON, Canada. [4]College of Environmental Sciences and Engineering, Peking University, Beijing, China.
*Corresponding author. Email: drew.gentner@yale.edu (D.R.G.); john.liggio@ec.gc.ca (J.L.)
†Present address: School of Engineering and Applied Sciences, Harvard University, Cambridge, MA, USA.
‡Present address: Department of Energy, Environmental, and Chemical Engineering, Washington University in St. Louis, St. Louis, MO, USA.
§Present address: Laboratory of Atmospheric Chemistry, Paul Scherrer Institute, AG-5232 Villigen, Switzerland.
¶Present address: Department of Civil and Environmental Engineering, Massachusetts Institute of Technology, Cambridge, MA, USA.
#Present address: Ramboll, Westford, MA, USA.

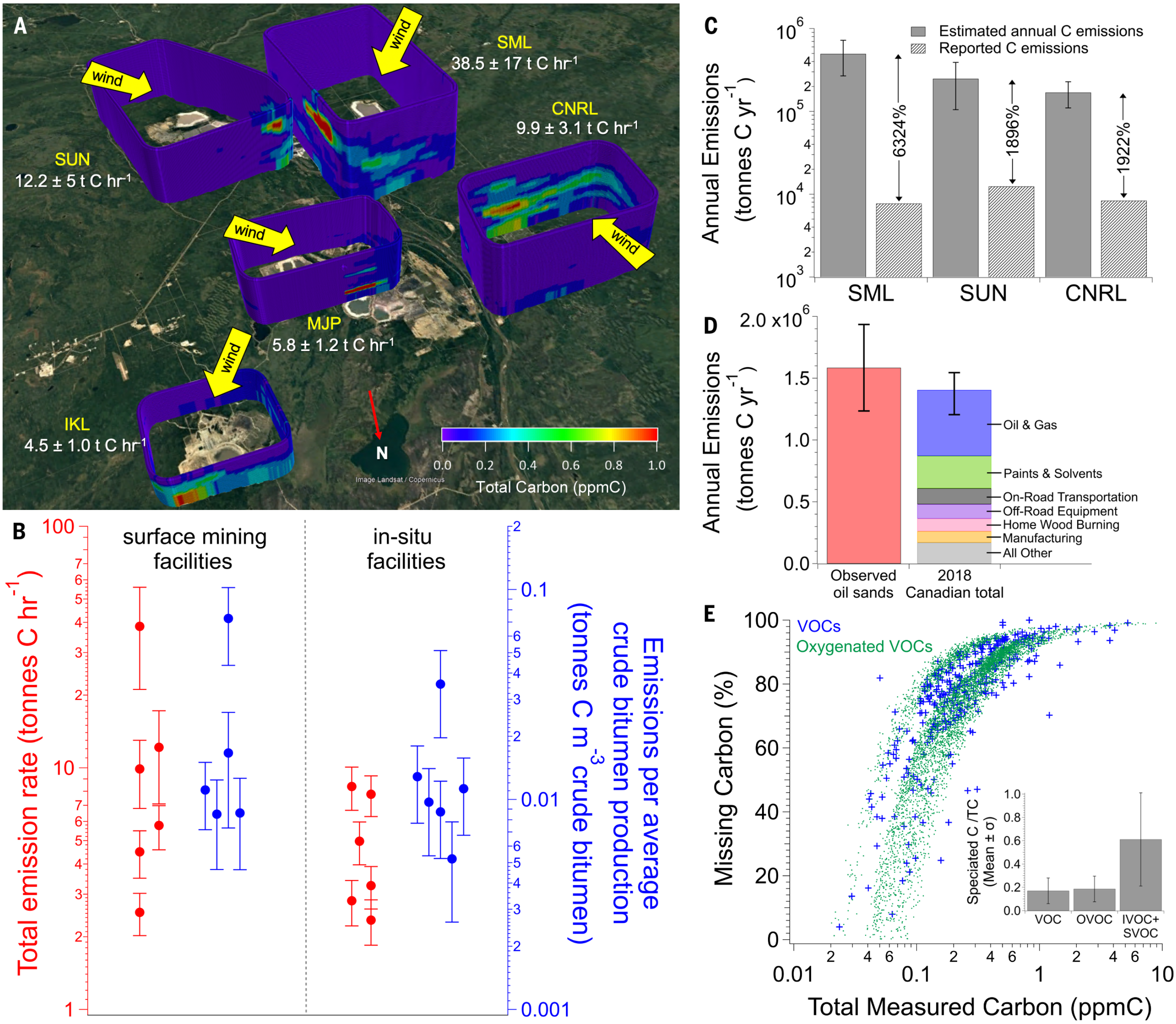

Fig. 1. Observed total gaseous organic carbon emissions, their hydrocarbon intensity, and comparisons with reported emissions. (**A**) Examples of box flights around five major surface mining facilities on different days show elevated downwind total gaseous organic carbon with total emissions derived with TERRA (supplementary materials, materials and methods). Numeric values in white indicate average TC emission rates. (**B**) Hourly carbon emission rates and average annual carbon intensities for surface mining and in situ facilities. Each marker indicates the mean for each site, and error bars indicate the standard deviation (number of flights per site is provided in fig. S3 and table S2). (**C**) Estimated annual gaseous organic carbon emissions compared with the reported emissions converted to carbon mass units for the three highest-emitting (both measured and reported) surface mining facilities (SML, SUN, and CNRL) (table S2), with percent differences. Annual emissions were estimated by using TC/NO_x ratios, and error bars indicate the standard deviation of the derived TC/NO_x ratios (with emissions derived as the TC/NO_x ratio scaled by reported annual NO_x emissions) (fig. S4 and supplementary materials). (**D**) Observed total gaseous organic carbon emissions for the studied facilities compared with the total Canadian annual inventory for 2018 converted to carbon units. (**E**) Percentage of "missing" organic carbon relative to either VOC or OVOC measurements based on canister samples, PTR-ToF-MS, and iodide-CIMS. (Inset) Average contributions of VOCs, OVOCs, and I/SVOCs to total observed organic carbon measurements in concentrated plumes (>0.35 ppmC), which represents the top 75th percentile of TC data. This is not in comparison with emissions inventories. For the purpose of comparing with the discrete speciated VOCs and OVOCs that are predominantly C_{10} and smaller, the IVOC+SVOC value in the inset is inclusive of C_{11} compounds.

sampled surface and in situ facilities was 0.024 ± 0.010 and 0.014 ± 0.006 tonnes C m^{-3} bitumen, respectively (Fig. 1B). These hydrocarbon intensities translate to total facility-wide emissions that are equivalent to 0.3 to 12.1% of production by mass (table S2), which is comparable with the magnitude of loss rates of highly volatile methane from US oil and gas operations (0.3 to 8.9%) (*24*). The magnitude of these emissions emphasizes the importance of total hydrocarbon measurements in capturing infrequently measured nonmethane organic compounds.

Total organic carbon annual emissions for facilities were estimated by using TC-to-NO_x (a combustion tracer) ratios multiplied by reported annual NO_x emissions (supplementary materials) (*25*, *26*), which has been performed for other pollutants (*27*–*29*). Emission ratios were obtained by means of empirical concentration correlations during box flights and TERRA-derived direct emission ratios (supplementary materials and fig. S5). The density of sources within facilities and nearby atmospheric mixing leads to both combustion and noncombustion gas-phase organic carbon sources being mixed and thus moderately correlated to NO_x in downwind measurements (fig. S5), which is similar in approach to well-correlated anthropogenic tracers downwind of major urban areas (*28*). Across the three highest-emitting facilities—Syncrude Mildred Lake (SML), Suncor (SUN), and Canadian Natural Resources (CNRL)—these average ratio values were 24 ± 11, 13 ± 7, and 17 ± 6 kg C (kg NO_x)$^{-1}$, respectively (Fig. 1C), yielding annual emissions estimates of ≈200,000 to 500,000 tonnes C year^{-1}. Although scaling with TC/NO_x is more robust than simple annual extrapolation (24 hours × 365 days), extrapolation remains within a factor of 2.2 on average (maximum 3), and both methods result in annual estimates far greater than reported emissions (table S2).

These large emission rates were 20 to 64 times greater than those in the Alberta Emissions Inventory Report (AEIR) and Canada's National Pollutant Release Inventory (NPRI), the latter of which is required to include the entire VOC-to-SVOC range for oil sands operations (Fig. 1C and tables S2 and S3). For context, the sum of measured gas-phase organic carbon emissions from all measured surface mining and in situ facilities in 2018 was 1.59×10^6 tonnes C year^{-1}, which is approximately equivalent to the VOC emissions reported for the sum of all anthropogenic sources in Canada's Air Pollutant Emissions Inventory (1.40×10^6 tonnes C year^{-1}) (carbon mass conversion is provided in the supplementary materials) (Fig. 1D) (*30*). Surveyed facilities included 88 and 50% of 2018 crude bitumen production from surface mining and in situ sites, respectively (table S2) (*23*, *31*). Thus, the oil sands sector alone represents a dominant fraction of country-wide gas-phase organic carbon emissions, even when only incuding the facilities studied here.

Measured VOCs only account for a fraction of total measured organic carbon (fig. S1), reflecting the need to report the full range of organic volatilities across oil sands and other anthropogenic sectors. Even when including measurements of oxygenated VOCs (OVOCs) with two on-board high-resolution mass spectrometers [proton transfer reaction–time of flight mass spectrometry (PTR-ToF-MS) and iodide–chemical ionization mass spectrometry (iodide-CIMS)] (table S4), a substantial fraction of carbon remains "missing" relative to the total carbon observations (Fig. 1E). In this case, "missing" indicates that the sum of speciated carbon is less than the total measured carbon. At lower total carbon concentrations (background air), most of the observed total carbon was speciated. In concentrated oil sands plumes with TC concentrations >0.35 ppmC, VOC and OVOC measurements were only responsible for 17 ± 11% and 19 ± 11% of carbon, respectively (Fig. 1E, inset). Conversely, the I/SVOCs observed in integrated low time-resolution adsorbent tube samples represented a greater fraction (61 ± 40%) (Fig. 1E and fig. S2), highlighting the abundant contributions of I/SVOCs to total oil sands–related emissions and their insufficient bottom-up quantification in reported emissions (table S3).

Abundant complex mixtures of oil sands–derived I/SVOCs near facilities

Time- and spatially integrated samples of I/SVOCs were collected during box flight segments (for example, Fig. 1A) and downwind transects and analyzed by means of gas chromatography on both unit-resolution and high-resolution mass spectrometers [gas chromatography–electron ionization–mass spectrometry (GC-EI-MS) and gas chromatography–time of flight (GC-ToF)], which revealed abundant complex mixtures of I/SVOCs near both surface mining and in situ facilities (Figs. 2 and 3). IVOCs (C_{12} to C_{18}) and SVOCs (C_{19} to C_{25}) were uncharacteristically abundant relative to VOCs (Fig. 1E) and were observed around various facilities, as shown in selected flight samples in Fig. 2A (additional examples are available in figs. S6 and S7). The relative abundances and composition varied between and around facilities, with maxima ranging from C_{17} to C_{22} (Fig. 2A, figs. S8 and S9, and tables S5 and S6), which may suggest varying on-site sources and emissions

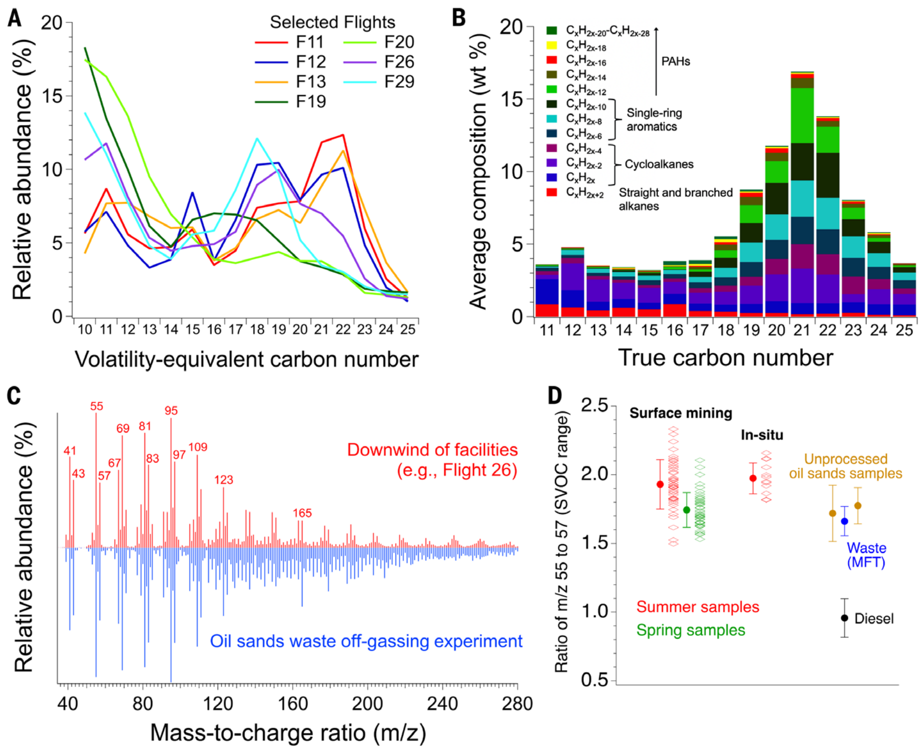

Fig. 2. Chemically speciated observations of abundant gas-phase I/SVOC mixtures near surface and in situ mining facilities are indicative of oil sands origin. (**A**) Relative volatility distributions of observed complex I/SVOC mixtures vary between facilities, shown as total ion chromatograms (across C_{10} to C_{25} by means of GC-EI-MS) in which each line is a sample from selected flights (other flights are available in fig. S6). (**B**) Average chemical composition of I/SVOC emissions across flight samples by means of high-resolution GC-ToF is consistent with the characteristics of oil sands bitumen indicating depleted acyclic (linear or branched) alkanes and relatively more mono-, bi-, and tri-cyclic alkanes. (**C**) SVOC mass spectra (by means of GC-EI-MS) from aircraft samples (flight 26) share similar characteristic mass spectral fragments with oil sands, including for multicyclic alkanes (for example, *m/z* 69, 81, 83, 95, 109, and 123), shown here with an average spectrum from oil sands MFT waste off-gassing experiments (Fig. 5). Flight 26 was chosen as an example with marked enhancement downwind of a concentrated area of facilities. (**D**) Average (±SD) of *m/z* 55/57 ratios measured with GC-EI-MS across all flight adsorbent tube samples (individual points) further demonstrates consistent reduced abundances of acyclic alkanes, shown with ratios from other oil sands materials (extractions of two types of unprocessed oil sands and MFT waste) and diesel fuel (*7*) for comparison.

pathways. There are stark differences in the observed concentrations when compared with that of urban areas. Average concentrations of primary gas-phase IVOCs were 6.3 ± 1.9 μg m^{-3} in greater Los Angeles, with primary gas-phase SVOC estimates of 0.6 μg m^{-3} (*1*). We observed average I/SVOC concentrations of 104 ± 93 μg m^{-3} (range, 10.2 to 409 μg m^{-3}) across flight samples, accompanied by corresponding total carbon enhancements (fig. S2).

Detailed chemical speciation of offline samples provided I/SVOC composition at the molecular formula level, with variations in I/SVOCs across samples (figs. S8 and S9). The average distribution based on all flight samples (Fig. 2B) exhibited a ~C_{20} to C_{22} maximum with aliphatic (alkane), single ring-aromatic, and polycyclic aromatic hydrocarbon (PAH) formulas comprising 43, 39, and 18% of the mass across the IVOC to SVOC range, respectively (Fig. 2B). These observed complex I/SVOC mixtures were consistent with the composition of oil sands materials in prior literature (*32*, *33*) and our own analysis of oil sands material samples (Fig. 2, C and D). This includes the large aromatic content substantially exceeding aliphatics in raw oil sands (*33*) and depleted levels of acyclic alkanes, with a large fraction of mono- through tetra-cyclic alkanes in the ~C_{15} to C_{23} range observed in Athabasca bitumen (*32*). Airborne measurements show relatively minor contributions from acyclic (linear or branched) alkanes, and prominent mass-to-charge (m/z) fragments associated with mono- and multicyclic alkanes (Fig. 2, B to D) (*34*). These cyclic-to-acyclic alkane ratios are elevated across flights and oil sands materials and are atypical of observations of common I/SVOC sources (such as diesel fuel combustion) (Fig. 2D) (*7*), further supporting that the observed I/SVOCs are oil sands–derived.

I/SVOC enhancements were often observed around and directly downwind of both surface mining and in situ facilities (Fig. 3). For example, flights 25 and 26 initially focused on a forest fire (*18*, *35*) upwind of oil sands operations, with the fifth screen, which was downwind of all major surface mining facilities, showing a marked enhancement in SVOC abundances and mass spectra indicative of oil sands–derived emissions (Figs. 2C and 3, A and B, and fig. S7B). The strong vertical gradient in screen 5′s transects (Fig. 3B) with higher SVOC abundances at lower altitudes implies ground-level emissions (<500 m). Enhancements were also observed directly downwind of in situ facilities (for example, flight 29) (Fig. 3, C and D), providing additional evidence of I/SVOC emissions from in situ operations.

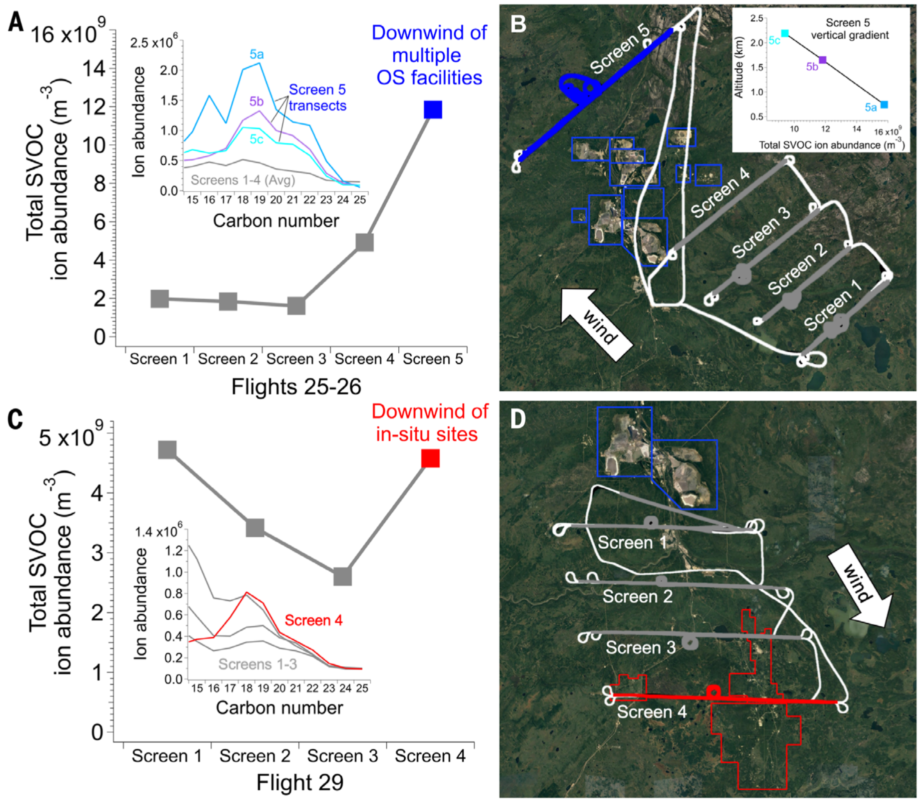

Fig. 3. Offline measurements of semivolatile organic compounds observed downwind of surface mining and in situ facilities. (**A**) Total SVOC ion abundances by using GC-EI-MS compared across upwind (screens 1 to 4) to downwind (screen 5) samples during consecutive flights 25 and 26. (Inset) The distribution of *n*-alkane volatility-equivalent C_{15}-to-C_{25} ion abundances (screen 5 samples are labeled 5a, 5b, and 5c, indicating different altitudes of the screen's transects above sea level). (**B**) Map of the five screens across flights 25 and 26, with screen 5 downwind of all surface mining facilities (outlined). (Inset) Vertical gradient with larger enhancements at lower altitudes for the three screen 5 transects. (**C**) Total SVOC ion abundances for flight 29 screens, in which screens 1 to 3 (gray) are downwind of surface mining facilities and screen 4 (red) is immediately downwind of multiple in situ facilities. (Inset) The distribution of C_{15}-to-C_{25} ion abundances. (**D**) Map of screens in flight 29 with outlined surface mining (blue) and in situ (red) facilities. Flights 25, 26, and 29 were conducted during daytime: flights 25 and 26, 8:45 to 17:20, and flight 29, 9:45 to 14:30, local time.

An important role for noncombustion carbon emissions

Measurements of TC were compared with established combustion tracers (NO_y; sum of all oxides of nitrogen). These TC/NO_y ratios were used to examine the relative contributions of organic carbon emitted from combustion-related (for example, vehicles and equipment) versus non–combustion-related sources (for example, evaporative and fugitive emissions). In addition to expected combustion-related emissions, there was clear evidence for substantial non–combustion-related emissions.

For example, flight 29's TC and NO_y measurements (Fig. 4A) show correlated enhancements across plume transects in screens 1 to 3 downwind of surface mining facilities (Fig. 3D), which is indicative of co-located emissions, although not necessarily co-emitted from the same on-site source(s). TC/NO_y ratios remained similar across the first three screens (~0.08 ppmC ppb^{-1}), with downwind transport and dilution of the plume from surface mining facilities. However, in screen 4, after intercepting emissions from the in situ facilities, the ratio increased to 0.19 ± 0.41 ppmC ppb^{-1}, with abundant TC enhancements from in situ facilities that were not correlated with NO_y, indicating that they were no longer co-located with combustion-related sources. The corresponding I/SVOC enhancements (Fig. 3, C and D) and spatially resolved analysis of screen 4 show clear TC enhancements at the lowest flight altitude (Fig. 4B and fig. S10), despite continued dilution of the upwind NO_y plume.

Elevated TC/NO_y ratios were also observed across other flights (flights 3, 4, 7 to 14, 17, 18, 20 to 22, 24, 29, and 30). The ratios are indicative of major contributions from non–combustion-related emissions pathways because they are substantially greater (≥10× on average) than the expected ratios from combustion-related sources (such as gasoline and diesel engines) in North American emissions inventories (Fig. 4C) (*30*, *36*). This necessitates further efforts to constrain both combustion and noncombustion sources at oil sands operations, including a broader consideration of organic carbon emissions (such as I/SVOCs).

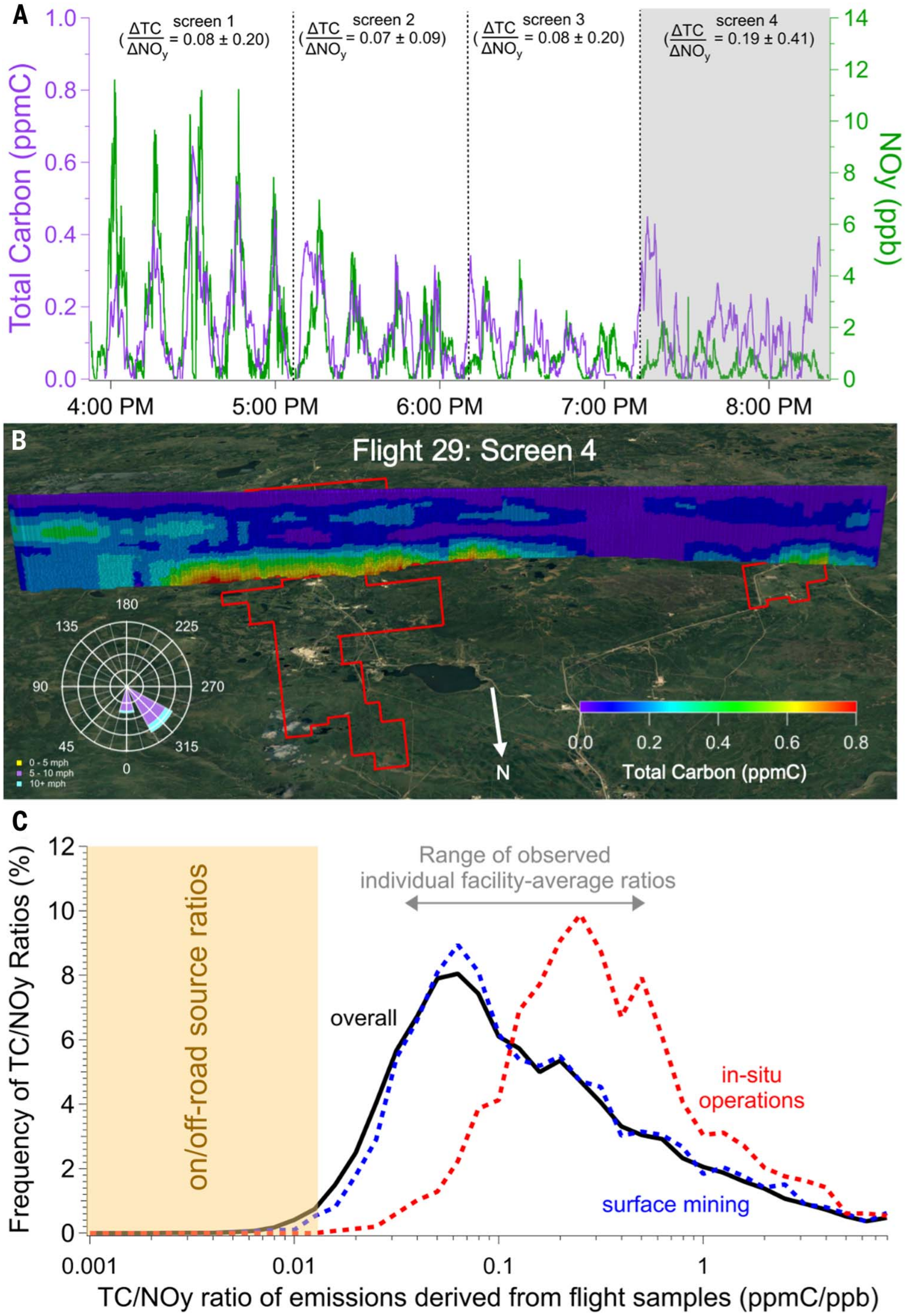

Fig. 4. Total gaseous organic carbon enhancements and their ratios to nitrogen oxide combustion tracers (NO_y) highlight the importance of non–combustion-related emissions. (**A**) Comparison of TC and NO_y background-subtracted concentrations across the four screens of flight 29, shown with average TC/NO_y ratios (above the 50th percentile). (**B**) Spatially resolved observations of TC corresponding to flight 29 screen 4 in (A) show enhancements in TC downwind of in situ facilities (red outline delineates Long Lake, Surmont, and JACOS Hangingstone) near ground level (Fig. 3C, map). Additional details on flight 29 can be found in the supplementary materials and figs. S10 and S11. (**C**) TC/NO_y ratios (10 s averages) across both facility types (solid black line), as well as flights around surface mining only (flights 11, 13, 20, 21, 22, 24, and 29, screens 1 to 3; dashed blue line) and in situ facilities only (flights 12, 18, and 29, screen 4; dashed red line). Background-subtracted concentrations above the 50th percentile within each data subset were used to focus the analysis on more concentrated plumes (>0.07 ppmC overall, >0.11 ppmC for surface mining only, and >0.06 ppmC for in situ only), with all data shown in figs. S12 and S13. The range of known ratios from on- and off-road sources (*30*, *36*) is shown for comparison. The surface mining and in situ distributions are not additive to the "overall" distribution, which encompasses additional flights.

Considering potential noncombustion emission pathways

Oil sands extraction and processing encompass multifaceted operations that vary with facility type, extraction methods, processing capabilities, and various on-site activities that may contribute to non–combustion-related emissions. Such I/SVOC emissions can be expected during mining operations from raw oil sands off-gassing and fugitive emissions during extraction and processing (*37*). Yet emissions may extend past processing stages, warranting holistic lifecycle-wide consideration of potential sources, including waste management. For example, tailings ponds are managed open pits that contain wastewater and by-products of the bitumen separation process, and off-gassing of I/SVOCs from tailings ponds has been hypothesized as a major source (*37*). However, available field measurement methods have been limited predominantly to VOCs (*3*, *15*), and the presence of water inhibits emissions owing to rate-limiting multiphase partitioning processes (*37*).

Decades of oil sands surface mining have resulted in large volumes of accumulated fluid tailings waste (water and solids), necessitating tailings reclamation measures to reduce the volume of tailings waste stored in ponds (*38*). We evaluated I/SVOC emissions from a tailings drying technique, which is used by the oil sands industry to process aged or fresh fine tailings. In 2018, 252 Mm^3 of treated fluid tailings were reported industry-wide (*38*). We specifically examined off-gassing emissions from mature fine tailings (MFT), an older mixture of fine particles (sand, silt, and clay) with residual bitumen that remains suspended in tailings ponds and is particularly difficult to separate from wastewater. Although several methods exist, we emulated atmospheric fines drying (also called thin lift drying or tailings reduction operations) through a series of bench-top experiments. Other methods such as accelerated drying techniques may vary. Yet all dried tailings (fine or coarse) are typically kept in either temporary storage areas, transferred to dedicated disposal areas, or used in construction projects (such as roads or dykes)—all of which are open to the atmosphere for some duration (*39*, *40*).

Although MFT off-gassing was initially relatively low, emissions increased markedly once the MFT were dry and remained elevated for weeks at environmentally relevant temperatures (Fig. 5A and table S7). Without the inhibiting water barrier, the diffusion of I/SVOCs through the dried MFT continued over the experiments' duration (up to 9 weeks), with increased emissions at higher surface temperatures and irradiation to simulate solar exposure (Fig. 5B and table S8). Whereas initial MFT off-gassing over the first 11 days included some VOCs (fig. S15), the emissions shifted toward the I/SVOC range after drying and aging and under increased

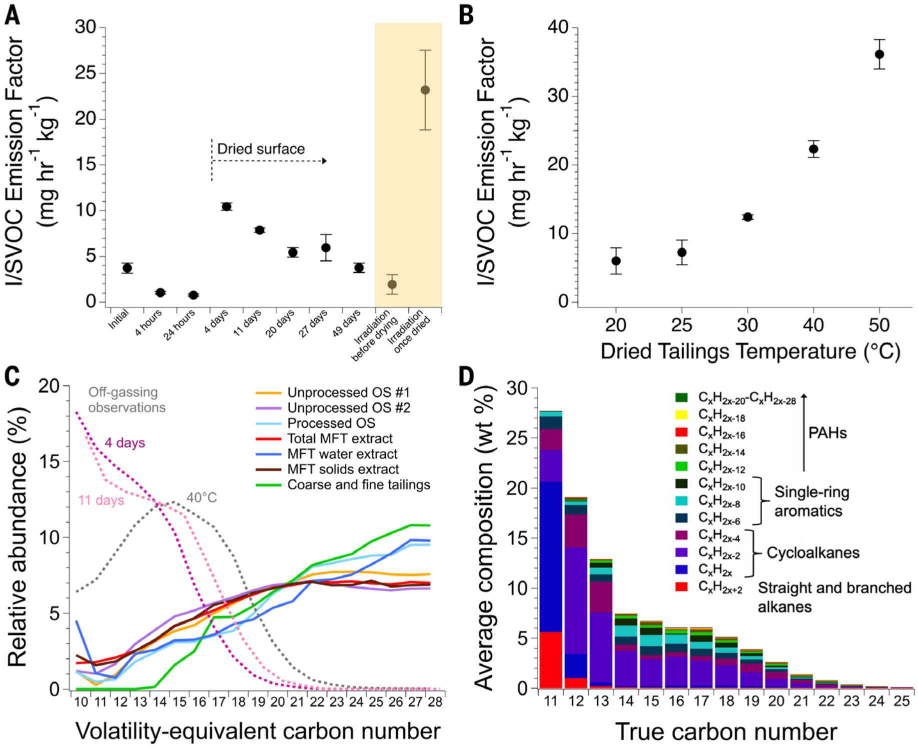

Fig. 5. Dried oil sands waste releases substantial quantities of I/SVOCs from hydrocarbon reservoirs sorbed to suspended tailings solids. (**A**) I/SVOC emission factors from MFT at various stages of drying-aging for an industry-supplied undried sample, and with irradiation of undried and dried tailings. (**B**) Temperature dependence of emissions from dried tailings [units in (A) and (B) are in *n*-alkane equivalent mass per mass of dry tailings, and error bars reflect emission factor SDs]. (**C**) Demonstration of underlying I/SVOC reservoirs in unprocessed oil sands, processed oil sands, and waste products as a function of *n*-alkane volatility-equivalent carbon number (by means of GC-EI-MS ion abundance). Examples of off-gassing emissions from MFT (including several days after application) are indicated with dashed lines for comparison. (**D**) Average I/SVOC composition observed in fresh and partially dried MFT off-gassing (samples both with and without irradiation at ~25°C are included here) by means of GC-TOF.

temperatures or irradiation (Fig. 5, A and B). The chemical speciation of MFT off-gassing emissions exhibits an enhancement in cyclic alkanes similar to that of ambient measurements, with characteristic fragments of multicyclic alkanes and limited acyclic alkanes (Figs. 2, C and D, and 5D; fig. S14; and table S9). The reservoir of I/SVOCs was not just present in MFT but was also observed in a range of materials spanning unprocessed oil sands, processed oil sands, and waste products (Fig. 5C). So although multiple similar on-site sources may exist, these observations show that tailings drying could be an important source of I/SVOCs, making substantial contributions to the total organic carbon observed in the flights.

Discussion

The magnitude of TC emissions observed from oil sands facilities far exceeds industry reports, with observed emissions [1.59 ± 0.35 million tonnes (Mt) C year^{-1}] being equivalent to the total Canadian anthropogenic emissions of organic carbon (Fig. 1, C and D). Total oil sands organic carbon emissions also far surpass reactive organic gas emissions from total anthropogenic sources (stationary, mobile, and chemical products) in the largest US megacities (such as Los Angeles) (~0.1 Mt C year^{-1} in the South Coast Air Basin) (*41*). These findings demonstrate that complete coverage of a wider volatility range of emissions is necessary to effectively inform science and policy because speciated VOC reporting alone is insufficient to capture the entire range of carbon emissions (Fig. 1, C and E, and fig. S2). Although oil sands operations are required to report “analytically unresolved hydrocarbon” (AUHC; including I/SVOCs), only a small number of operators reported such emissions in 2018, with negligible contributions to total reported organic carbon (0 to 2.6 × 10^{-3} Mt C year^{-1}) in 2018 (*42*). In subsequent years, reported AUHC has increased in magnitude (up to 1.5 × 10^{-2} Mt C year^{-1} in 2021) yet remain a minor contributor (~1%) to total measured emissions. Given that I/SVOCs are estimated to represent ~60% of carbon in concentrated plumes (Fig. 1E), the full air quality and environmental impacts of oil sands operations cannot be evaluated without more realistic inclusion of IVOCs and SVOCs in emissions reporting.

Although a diverse range of on-site sources—including from extraction, processing, and tailings ponds (*37*)—likely contributes to the observed total organic carbon emissions from surface mining facilities, our laboratory experiments identified potential unintended consequences of tailings reduction strategies to reduce the volumes of tailings water. This warrants further measurements and consideration of off-gassing emissions resulting from oil sands waste management strategies, especially given that the dewatering of tailings by means of a variety of other forced-drying techniques will similarly produce dried solids without an inhibiting water layer. Although not currently considered a VOC-SVOC source, this is a timely issue because the surface area of nonfluid tailings in the oil sands has grown considerably with increased oil sands production over the past several decades, with 119 km^2 (in 2020) representing 40% of total waste surface area (*43*). Hence, the potential for dried waste products to emit large amounts of reactive I/SVOCs to the atmosphere suggests that reducing liquid waste by such methods opens up potentially large and unexpected pathways of atmospheric pollution.

Prior work has focused on surface mining operations, but total gaseous organic carbon emissions from in situ facilities also greatly exceed reported emissions. With total carbon emissions per bitumen production (hydrocarbon intensity) comparable with that of surface mining (Fig. 1B), further examination of their emissions is warranted because the proportion of bitumen production from in situ extraction will increase beyond ~50% over the coming decade (*13*).

Effective emissions mitigation to achieve cobenefits across air quality–, health-, climate-, and energy-related goals requires accurate representation in inventories. This cannot be accomplished without the combination of both bottom-up and top-down approaches to examine closure and reveal emissions that require further scrutiny. In the case of both oil sands operations and many other anthropogenic sources, routinely monitoring all gas-phase organic carbon emissions with complete speciation is often infeasible for researchers, operators, and regulators. For I/SVOCs, the challenges associated with measuring their inherently complex mixtures demonstrate how total organic carbon observations would enable inclusive, routine carbon coverage across an anthropogenically ubiquitous class of compounds that drive secondary organic $PM_{2.5}$ formation (*7*, *8*, *44*, *45*). The total organic carbon approach here can also be a valuable tool used to capture a broader range of chemical species across the VOC-SVOC range, thus identifying the presence of previously unknown hydrocarbons or functionalized organic compounds, unknown or underconstrained sources, spatiotemporally variable emissions, hotspots, or noncompliance. This facilitates the quantification of sources in emissions inventories and the modeling of their contributions to both primary hazardous pollutant concentrations and to secondary pollutant formation. Future applications can similarly improve emissions reporting across many other anthropogenic sources and locations because accounting for life cycle wide emissions of chemically diverse compound classes by means of total carbon monitoring presents a vastly simpler approach with inherent mass closure checks for industry, scientists, and policy-makers alike.

REFERENCES AND NOTES

1. Y. Zhao *et al*., *Environ. Sci. Technol.* **48**, 13743–13750 (2014).
2. E. N. Kelly *et al*., *Proc. Natl. Acad. Sci. U.S.A.* **106**, 22346–22351 (2009).
3. I. J. Simpson *et al*., *Atmos. Chem. Phys.* **10**, 11931–11954 (2010).
4. J. L. Jimenez *et al*., *Science* **326**, 1525–1529 (2009).
5. S. Feng, D. Gao, F. Liao, F. Zhou, X. Wang, *Ecotoxicol. Environ. Saf.* **128**, 67–74 (2016).
6. S. Fuzzi *et al*., *Atmos. Chem. Phys.* **15**, 8217–8299 (2015).
7. D. R. Gentner *et al*., *Proc. Natl. Acad. Sci. U.S.A.* **109**, 18318–18323 (2012).
8. Q. Lu, Y. Zhao, A. L. Robinson, *Atmos. Chem. Phys.* **18**, 17637–17654 (2018).
9. G. Pétron *et al*., *J. Geophys. Res. Atmos.* **119**, 6836–6852 (2014).
10. J. Liggio *et al*., *Nature* **534**, 91–94 (2016).
11. L. Rosa, K. F. Davis, M. C. Rulli, P. D'Odorico, *Earths Futur.* **5**, 158–170 (2017).
12. Government of Alberta, "Environmental management of Alberta's oil sands" (2009); https://open.alberta.ca/publications/9780778576778.
13. Alberta Energy Regulator, "Crude Bitumen - In Situ Production" (2023); https://www.aer.ca/providing-information/data-and-reports/statistical-reports/st98/crude-bitumen/production/in-situ.
14. Alberta Energy Regulator, "ST3: Alberta Energy Resource Industries Monthly Statistics" (2017); https://www.aer.ca/providing-information/data-and-reports/statistical-reports/st3.
15. S. M. Li *et al*., *Proc. Natl. Acad. Sci. U.S.A.* **114**, E3756–E3765 (2017).
16. J. Liggio *et al*., *Atmos. Chem. Phys.* **17**, 8411–8427 (2017).
17. J. R. Brook *et al*., *J. Air Waste Manag. Assoc.* **69**, 661–709 (2019).
18. K. L. Hayden *et al*., *Atmos. Chem. Phys.* **22**, 12493–12523 (2022).
19. M. Gordon *et al*., *Atmos. Meas. Tech.* **8**, 3745–3765 (2015).
20. J. Liggio *et al*., *Nat. Commun.* **10**, 1863 (2019).
21. B. M. Erland *et al*., *Atmos. Meas. Tech.* **15**, 5841–5859 (2022).
22. A. D. Charpentier, J. A. Bergerson, H. L. MacLean, *Environ. Res. Lett.* **4**, 014005 (2009).
23. Alberta Energy Regulator, "Statistical Series 39 Alberta Mineable Oil Sands Plant Statistics Monthly Supplement" (2018); https://static.aer.ca/prd/documents/sts/ST39-2018.pdf.
24. J. Peischl *et al*., *J. Geophys. Res. Atmos.* **123**, 7725–7740 (2018).
25. Environment and Climate Change Canada, "National Pollutant Release Inventory" (2019); https://pollution-waste.canada.ca/national-release-inventory/archives/index.cfm?lang=en.
26. Government of Alberta, "Alberta Emissions Inventory Report (AEIR) Air Emission Rates" (2020); https://open.alberta.ca/opendata/aeiraiemissionrates#summary.
27. I. B. Konovalov *et al*., *Atmos. Chem. Phys.* **16**, 13509–13540 (2016).
28. F. Liu *et al*., *Atmos. Chem. Phys.* **20**, 99–116 (2020).
29. S. N. Wren *et al*., *PNAS Nexus* **2**, pgad140 (2023).
30. Environment and Climate Change Canada, "Canada's Air Pollutant Emissions Inventory" (2018); https://data-donnees.ec.gc.ca/data/substances/monitor/canada-s-air-pollutant-emissions-inventory.
31. Alberta Energy Regulator, "ST53: Alberta In Situ Oil Sands Production Summary" (2018); https://www.aer.ca/providing-information/data-and-reports/statistical-reports/st53.
32. O. P. Strausz *et al*., *Energy Fuels* **24**, 5053–5072 (2010).
33. L. He, X. Li, G. Wu, F. Lin, H. Sui, *Energy Fuels* **27**, 4677–4683 (2013).
34. M. H. Erickson, M. Gueneron, B. T. Jobson, *Atmos. Meas. Tech.* **7**, 225–239 (2014).
35. J. C. Ditto *et al*., *Atmos. Chem. Phys.* **21**, 255–267 (2021).
36. California Air Resources Board, "2015 Estimated Annual Average Emissions Statewide" (2016); https://www.arb.ca.gov/app/emsinv/2017/emseic1p_query.php.
37. B. D. Drollette, D. R. Gentner, D. L. Plata, *Environ. Sci. Technol.* **54**, 9872–9881 (2020).
38. Alberta Energy Regulator, "State of Fluid Tailings Management for Mineable Oil Sands, 2020" (2021); https://static.aer.ca/prd/documents/reports/2020-State-Fluid-Tailings-Management-Mineable-OilSands.pdf.
39. Canadian Natural Upgrading, "Canadian Natural Muskeg River Mine Fluid Tailings Management Report" (Canadian Natural Upgrading, 2020); https://www.aer.ca/providing-information/by-topic/tailings.
40. Alberta Energy Regulator, "State of Fluid Tailings Management for Mineable Oil Sands, 2018" (2019); https://static.aer.ca/prd/documents/oilsands/2018-State-Fluid-Tailings-Management-Mineable-OilSands.pdf.
41. California Air Resources Board, "CEPAM2019v1.03 Emission Projection Data 2017: Estimated Annual Average Emissions Los Angeles County" (2017); https://ww2.arb.ca.gov/applications/emissions-county.
42. Environment and Climate Change Canada, "2018 National Pollutant Release Inventory (NPRI) Facility-Reported Data" (2018); https://www.canada.ca/en/services/environment/pollution-waste-management/national-pollutant-release-inventory.html.
43. G. Chow-Fraser, A. Rougeot, *50 Years of Sprawling Tailings: Mapping Decades of Destruction by Oil Sands Tailings* (CPAWS Northern Alberta, Environmental Defence Canada, 2022).
44. B. A. Nault *et al*., *Atmos. Chem. Phys.* **21**, 11201–11224 (2021).
45. A. Hodzic *et al*., *Atmos. Chem. Phys.* **10**, 5491–5514 (2010).

ACKNOWLEDGMENTS

The authors acknowledge the substantial technical and scientific contributions toward the success of this study from the AQRD technical and data teams, the NRC team, and the leadership of S. Cober. We thank A. Goldstein and R. Harley (UC Berkeley) for the use of the diesel fuel composition data used in Fig. 2D. **Funding:** J.C.D., M.H., L.G., J.M., T.N.H.-M., C.C., P.K., and D.R.G. acknowledge support from the National Science Foundation (AGS-1764126 and CBET-2011362) and GERSTEL for their collaboration with the thermal desorption unit used as part of this study, and M.H. also acknowledges the Goldwater Scholarship Foundation. S.-M.L. acknowledges the support of the Ministry of Science and Technology of China (grant 2019YFC0214700). The project was partially funded by Environment and Climate Change Canada's Climate Change and Air Pollutants Program. This work was also partially funded under the OSM program, and the results are independent of any position of the program. **Author contributions:** Conceptualization: D.R.G., J.L., and S.-M.L. Methodology: J.L., D.R.G., and S.-M.L. Investigation: All authors. Visualization: M.H., D.R.G.., J.L., J.C.D., and L.G. Supervision: D.R.G., J.L., S-M.L., and J.C.D. Writing – original draft: M.H. Writing – review and editing: J.L., D.R.G., M.H., and all authors. **Competing interests:** The authors declare no competing interests in this study. **Data availability:** Flight campaign data are publicly available at https://donnees.ec.gc.ca/data/air/monitor/ambient-air-quality-oil-sands-region/pollutant-transformation-aircraft-based-multi-parameters-oil-sands-region/?lang=en. Other data and analysis relevant to the interpretation of the results can be found in the supplementary materials.

SUPPLEMENTARY MATERIALS

science.org/doi/10.1126/science.adj6233
Materials and Methods
Supplementary Text
Figs. S1 to S15
Tables S1 to S10
References (*46–70*)

Submitted 13 July 2023; accepted 15 December 2023
10.1126/science.adj6233